Large CO_2 effluxes at night and during synoptic weather events significantly contribute to CO_2 emissions from a reservoir

2016 Environ. Res. Lett. 11 064001

(http://iopscience.iop.org/1748-9326/11/6/064001)

Environmental Research Letters

OPEN ACCESS

RECEIVED
16 March 2015

REVISED
30 March 2016

ACCEPTED FOR PUBLICATION
6 May 2016

PUBLISHED
24 May 2016

LETTER

Large CO_2 effluxes at night and during synoptic weather events significantly contribute to CO_2 emissions from a reservoir

Heping Liu[1], Qianyu Zhang[1], Gabriel G Katul[2], Jonathan J Cole[3], F Stuart Chapin III[4] and Sally MacIntyre[5]

[1] Department of Civil and Environmental Engineering, Washington State University, Pullman, WA 99164, USA
[2] Nicholas School of the Environment, Duke University, Durham, NC 27708, USA
[3] Cary Institute of Ecosystem Studies, Box AB, Millbrook, NY 12545, USA
[4] Institute of Arctic Biology, University of Alaska Fairbanks, Fairbanks, AK 99775, USA
[5] Department of Ecology, Evolution, and Marine Biology, University of California, Santa Barbara, CA, USA

E-mail: Heping.Liu@wsu.edu

Keywords: carbon emissions from lakes, eddy covariance flux of CO_2, wind-based gas transfer, lake-atmosphere interactions

Supplementary material for this article is available online

Abstract

CO_2 emissions from inland waters are commonly determined by indirect methods that are based on the product of a gas transfer coefficient and the concentration gradient at the air water interface (e.g., wind-based gas transfer models). The measurements of concentration gradient are typically collected during the day in fair weather throughout the course of a year. Direct measurements of eddy covariance CO_2 fluxes from a large inland water body (Ross Barnett reservoir, Mississippi, USA) show that CO_2 effluxes at night are approximately 70% greater than those during the day. At longer time scales, frequent synoptic weather events associated with extratropical cyclones induce CO_2 flux pulses, resulting in further increase in annual CO_2 effluxes by 16%. Therefore, CO_2 emission rates from this reservoir, if these diel and synoptic processes are under-sampled, are likely to be underestimated by approximately 40%. Our results also indicate that the CO_2 emission rates from global inland waters reported in the literature, when based on indirect methods, are likely underestimated. Field samplings and indirect modeling frameworks that estimate CO_2 emissions should account for both daytime–nighttime efflux difference and enhanced emissions during synoptic weather events. The analysis here can guide carbon emission sampling to improve regional carbon estimates.

1. Introduction

The significance of inland waters to regional and global carbon cycles is rarely disputed (Cole *et al* 2007, Battin *et al* 2009, Raymond *et al* 2013). The total CO_2 and CH_4 emissions from inland waters are estimated at 2.1 Pg C yr^{-1} and 0.65 Pg C yr^{-1}, respectively (Cole *et al* 2007, Bastviken *et al* 2011, Raymond *et al* 2013). CO_2 emissions from inland waters are a consequence of the super-saturation of CO_2 in the surface water, as quantified by CO_2 concentration in the surface water (hereafter pCO_2) (Cole *et al* 1994, Sobek *et al* 2005). Such super-saturation is primarily due to respiration of allochthonous organic carbon and transport to aquatic systems of dissolved CO_2 by surface runoff and ground water flows (Kling *et al* 1991, Cole *et al* 2007). CO_2 emission rates are conventionally estimated by indirect methods (e.g., wind-based gas transfer models and the surface renewal model) that rely on pCO_2 and a gas transfer coefficient (hereafter indirect methods) (Cole *et al* 1994, 2010).

Therefore, one major focus has been on ways that biotic and abiotic processes affect pCO_2 and thus CO_2 emissions. Recent studies found that lake CO_2 fluxes, directly measured by eddy covariance, can be weakly or entirely uncorrelated with water pCO_2 at short time scales (Aberg *et al* 2010), suggesting that physical processes within the water column mediate CO_2 emissions. Another major focus has been on reducing the uncertainty in quantifying the gas transfer coefficient (e.g., Cole *et al* 2010, MacIntyre *et al* 2010, Raymond *et al* 2013). Widely used models of the gas exchange coefficient are parameterized with empirical relations that depend upon mean wind speed (Cole *et al* 2010).

Rates of CO_2 transfer across the water-atmosphere interface may also be governed by physical processes other than wind speed in the low to intermediate wind speed regimes (e.g., Eugster *et al* 2003, McGillis *et al* 2004, Zappa *et al* 2004, Jeffery *et al* 2007, MacIntyre *et al* 2010, Rutgersson and Smedman 2010, Rutgersson *et al* 2011). Since different processes co-regulate CO_2 exchange across the water-air interface, it is expected that these processes exert varying levels of controls on different time scales, leading to temporal variations in CO_2 emission rates.

Temporally discrete field samplings of pCO_2 and atmospheric CO_2 concentrations for estimating CO_2 emission rates are usually conducted during daytime when fair weather conditions predominate, and these emission rates are then temporally up-scaled to obtain annual emission rates (Cole *et al* 2007, Raymond *et al* 2013). This temporally discrete sampling strategy, widely used in quantifying gas transfer across the water-atmosphere interface, does not account for nighttime–daytime emission differences and emissions during periods between samplings. The time-continuous eddy covariance method and the temporally up-scaled wind-based gas transfer method result in substantial discrepancies in annual CO_2 emission estimates (Jonsson *et al* 2008, Huotari *et al* 2011), raising questions about the currently reported CO_2 emission rates from global inland waters (Raymond *et al* 2013). Resolving this issue by identifying the sources of uncertainties and understanding underlying mechanisms is necessary for reducing uncertainties in the contribution of carbon emissions from global inland waters in regional and global carbon budgets and the response of inland waters to climate change (Cole *et al* 2007, Battin *et al* 2009, Tranvik *et al* 2009, Raymond *et al* 2013).

Here, half-hourly eddy covariance data of CO_2 fluxes and other microclimate variables over a 1-year period in 2008 over a large reservoir in Mississippi are analyzed and presented. Our objectives are to characterize variations in CO_2 fluxes across the water-atmosphere interface on diurnal and seasonal time scales, and demonstrate the significance of such diurnal variations and sub-seasonal events in CO_2 effluxes when upscaling to annual CO_2 emission estimates.

2. Site, instruments, and methods

The Ross Barnett Reservoir is located in central Mississippi (32°26′N, 90°02′W), USA, and has a surface area of about 134 km^2 and water depths varying from 4 to 8 m. The construction of the reservoir was completed in 1963. The main purpose of the reservoir is to provide a permanent water source to supply drinking water for the Mississippi capital city of Jackson. Water is monitored and controlled from an electrical/mechanical spillway and gate system in its southern shore by releasing water into the Pearl River. The reservoir is ice-free year round. A 5 m tower (Climatronics Corp.) was constructed over a stationary wooden platform in the south center of the reservoir, with the mean water depth around the tower of about 5 m and the distance from the tower to the shore ranging from 2 km to more than 14 km (Liu *et al* 2009, 2011, 2012, Zhang and Liu 2013, 2014). An eddy covariance system at a height of 4 m above the water surface was installed to measure CO_2 fluxes. The system consisted of a three-dimensional sonic anemometer (model CSAT3, Campbell Scientific, Inc.) and an open path CO_2/H_2O infrared gas analyzer (IRGA; Model LI-7500, LI-COR, Inc.). Three-dimensional wind velocity components and sonic virtual temperature from the sonic anemometer and densities of carbon dioxide and water vapor from the IRGA were recorded by a datalogger (model CR5000, Campbell Scientific, Inc.) at a frequency of 10 Hz.

Other microclimate variables were also measured as 30 min averages with 1 s readings, including net radiation (Rn) at 1.2 m (model Q-7.1, Radiation and Energy Balance Systems, Campbell Scientific, Inc.), air temperature (T_a) and relative humidity (RH) (model HMP45C, Vaisala, Inc.) at 1.9, 3.0, 4.0, and 5.5 m, wind speeds (U) and wind direction (WD) (model 03001, RM Young, Inc.) at 5.5 m. The water skin temperature (T_s) was measured by an infrared temperature sensor (model IRR-P, Apogee, Inc.). Vapor pressure on the water surface (e_s) was calculated as the saturation vapor pressure at the infrared-determined T_s. Water temperatures at eight depths of 0.10, 0.25, 0.5, 1.0, 1.5, 2.5, 3.5, and 4.5 m below the water surface were measured at 1 min interval and then integrated into 30 min mean values by eight water temperature probes (model 107-L, Campbell Scientific, Inc.), all tied to a buoy. The 107-L sensors have Steinhard-Hart equation errors of less than ± 0.01 °C. We did an internal correction on the sensors, which had accuracy of order 0.2 °C, based on the assumption that nocturnal mixing would cause uniform temperatures near midnight. Instrument drift led to residual errors on the order of 0.1 °C. Half-hourly precipitation totals were measured using an automated tipping-bucket rain gauge (model TE525, Texas Instruments, Inc.). All instruments were powered by six deep-cycle marine batteries that were charged by two solar panels (model SP65, 65 Watt Solar Panel, Campbell Scientific, Inc.).

The post-field data processing program was developed following FLUXNET's standard procedures and has been used in previous studies (Liu *et al* 2009, 2011, 2012, Zhang and Liu 2013, 2014) (see supplementary materials: note S1). After quality control and quality assurance (QA/QC), the 30 min time-series eddy covariance CO_2 flux in 2008 is shown in supplementary figure S1.

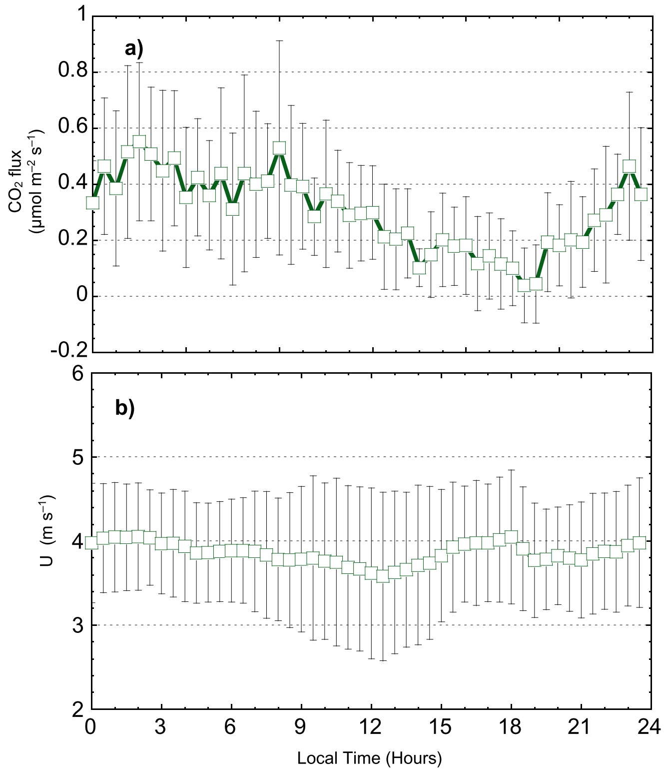

Figure 1. Annually averaged diurnal variations of atmospheric variables. (a) CO_2 flux: eddy covariance CO_2 flux (μmol^{-1} m^{-2} s^{-1}) with its standard deviation. (b) *U*: mean wind speeds (m s^{-1}) with its standard deviation. Monthly averaged diurnal variations of various variables are provided in supplementary figure 2. The daytime is defined as the 12 h period from 08:00 to 20:00 LT in this study.

3. Results and discussion

3.1. Diurnal variations in CO_2 efflux and their influence on CO_2 emissions

Monthly and annually averaged diurnal variations of CO_2 fluxes showed overall larger CO_2 effluxes at night than during the day, with the daily maxima in the early mornings and the minima in the late afternoons (figure 1, supplementary figure S3). The mean CO_2 effluxes during the nighttime (0.39 μmol m^{-2} s^{-1}) over the 1-year period of 2008 were approximately 70% larger than those during the daytime (defined as the 12 h period from 08:00 to 20:00 LT) (0.23 μmol m^{-2} s^{-1}) at a 95% significance level, resulting in the annual daily mean (i.e., 24 h average) efflux of 0.31 μmol m^{-2} s^{-1}. Therefore, the daytime mean efflux was 26% smaller than the daily mean efflux on an annual basis. Field samplings of aquatic pCO_2 for estimating CO_2 emissions are commonly conducted during the daytime when eddy covariance CO_2 efflux measurements report lower values than at night. This sampling bias in timing inherent in reported fluxes from indirect methods here underestimates the annual daily mean efflux by 26%, as compared with the time-integrated eddy covariance measurements. It should be noted that this bias is strictly due to the choice of sampling times of aquatic pCO_2 when estimating CO_2 emission rates and is not related to any particular formulation of gas transfer or measurement uncertainty in aquatic pCO_2.

A variety of biotic and abiotic controls contributed to the greater gas emissions at night than during the day. In the reservoir, the mean pH, dissolved oxygen, and oxygen saturation were 8.0, 7 mg L^{-1}, and 91%, respectively (Wersal *et al* 2006). Chlorophyll-α varied from 5 to 15 μg L^{-1} chl-α in the summer months (May, June, and July) (Wersal *et al* 2006, Sobolev *et al* 2009). It was observed that the upper water layer from 0–0.5 m was supersaturated with oxygen of 105%–144%; whereas the deeper water layer was undersaturated with oxygen decreasing to 30% (Wersal *et al* 2006). The pH values also decreased with depth, varying from 9.4–6.9. These observations reflect primary production in the upper water column and respiration in the deeper water layers. Thus, the primary production was likely to have caused a decrease in pCO_2 in the upper water column during the day. During winter, the water column tended to be well mixed to the depth of the deepest temperature sensor. However, when wind directions changed, near surface temperatures sometimes increased, and temperatures in the lower water column decreased. The former is indicative of advection, and the latter indicates a reservoir of cooler water at depth, which, based on the attributes of the reservoir, was likely enriched in pCO_2. Nocturnal cooling would have entrained this water to the surface and contributed to the higher

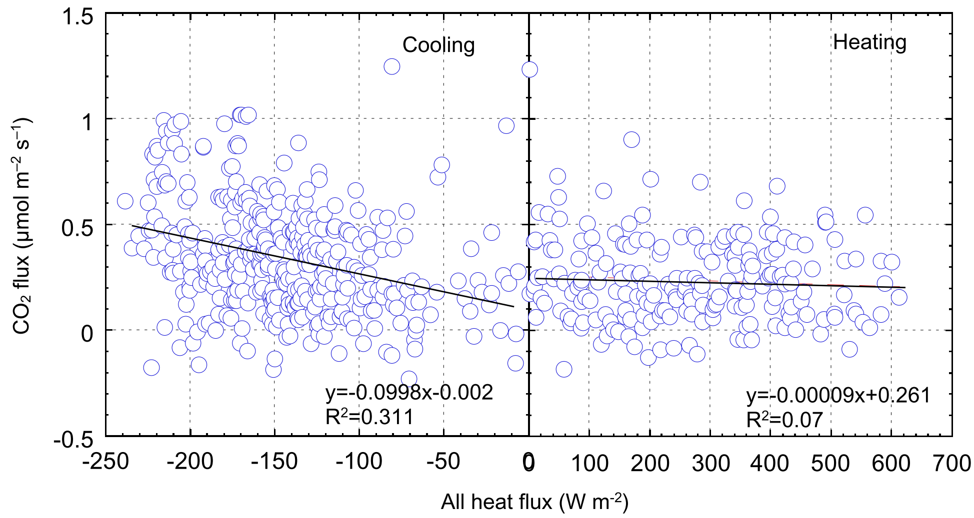

Figure 2. Linear regressions between CO_2 fluxes and all heat fluxes during the cooling period (left panel) and between CO_2 fluxes and all heat fluxes during the heating period (right panel) with the same datasets used in figure 1. Negative heat flux denotes that the water surface loses heat to the atmosphere.

nocturnal CO_2 fluxes (supplementary figure S4). During summer the daytime water column was thermally stratified. As winds picked up at night, the depth of the diurnal thermocline deepened and temperatures became uniform to the depth of the deepest sensor. On relaxation of the wind the following morning, cool water was again found at those depths. We computed the Wedderburn number, $W = \frac{g}{\rho_w}\Delta\rho_w\, h^2/(u_{*w}^2 L_f)$, which quantifies the relative significance of the buoyancy force in the water to the shear stress at the water-atmosphere interface (Imberger and Patterson 1990, MacIntyre *et al* 2009a). Here, g is gravitational acceleration, ρ_w is the water density, h is the mixed layer depth, u_{*w} is water friction velocity computed from the air and water densities and measured u_* in air assuming the dynamic shear stress is equivalent on both sides of the air-water interface, and L_f is the effective horizontal length of the lake along the line of fetch. The Wedderburn numbers were of order 10 during the day (i.e. strong vertical stratification with minimal thermocline upwelling) and 1 at night (full water column upwelling and vertical mixing such that associated horizontal scale of variability in CO_2 concentrations cannot be ignored) (supplementary figure S5). Thus, in summer, the increased CO_2 fluxes at night would have resulted from the combination of convective mixing (Crill *et al* 1988), mixing associated with internal wave motions at low Wedderburn number (MacIntyre *et al* 2009b), and spatial variability of CO_2 in the footprint (Heiskanen *et al* 2014). CO_2 fluxes tended to be somewhat higher with lower values of u_* and U. In summer, the winds tend to increase near mid-night and then decrease while winds were still changing direction. The independence of CO_2 fluxes from wind speed thus likely results from modifications of the related changes in concentration of CO_2 in the footprint as winds changed direction. The relation between CO_2 fluxes, the total heat budget in the water surface, plus our calculations of the Wedderburn number (supplementary figure S5), indicates that heat loss and wind induced processes occurring at night explained approximately 31% of the variability in CO_2 efflux (figure 2). CO_2 effluxes slightly declined with the enhanced heating of the mixed layer in the day (figure 2).

3.2. CO_2 flux pulses and their contribution to CO_2 emissions

The seasonal measurements indicate that the diurnal variations of CO_2 effluxes were superimposed by large CO_2 flux pulses that occurred occasionally throughout the year. As shown by a CO_2 flux pulse example from April 11 to 16 (figure 3), each of these CO_2 flux pulses persisted for up to a few days. These pulses, accompanied mostly by sensible and latent heat flux pulses (hereafter H and LE pulses), were caused directly by high-wind events associated with synoptic weather activities such as passages of extratropical cyclones with windy, cold/cool, dry air masses immediately behind them (Liu *et al* 2009, Zhang and Liu 2013). In the analysis here, a 'flux pulse' is defined as occurring when the 24 h mean fluxes exceed 1.5 times the centered 10-day running mean (Liu *et al* 2009, Zhang and Liu 2013). The CO_2 flux pulses were taken to be the same periods as H and LE pulses. By examining synoptic weather charts for consecutive days (www.wpc.ncep.noaa.gov/dailywxmap/), we were able to verify that such pulse events were caused by synoptic weather events associated with cold front passages. As shown in figure 3, the cyclone passed over the site at about 12:00 LT on April 11, resulting in a shift in wind directions from southerly winds to northwesterly winds, an increase in wind speeds from 4 to 10 m s^{-1}, and a decrease in air temperature from 24 °C to 6 °C

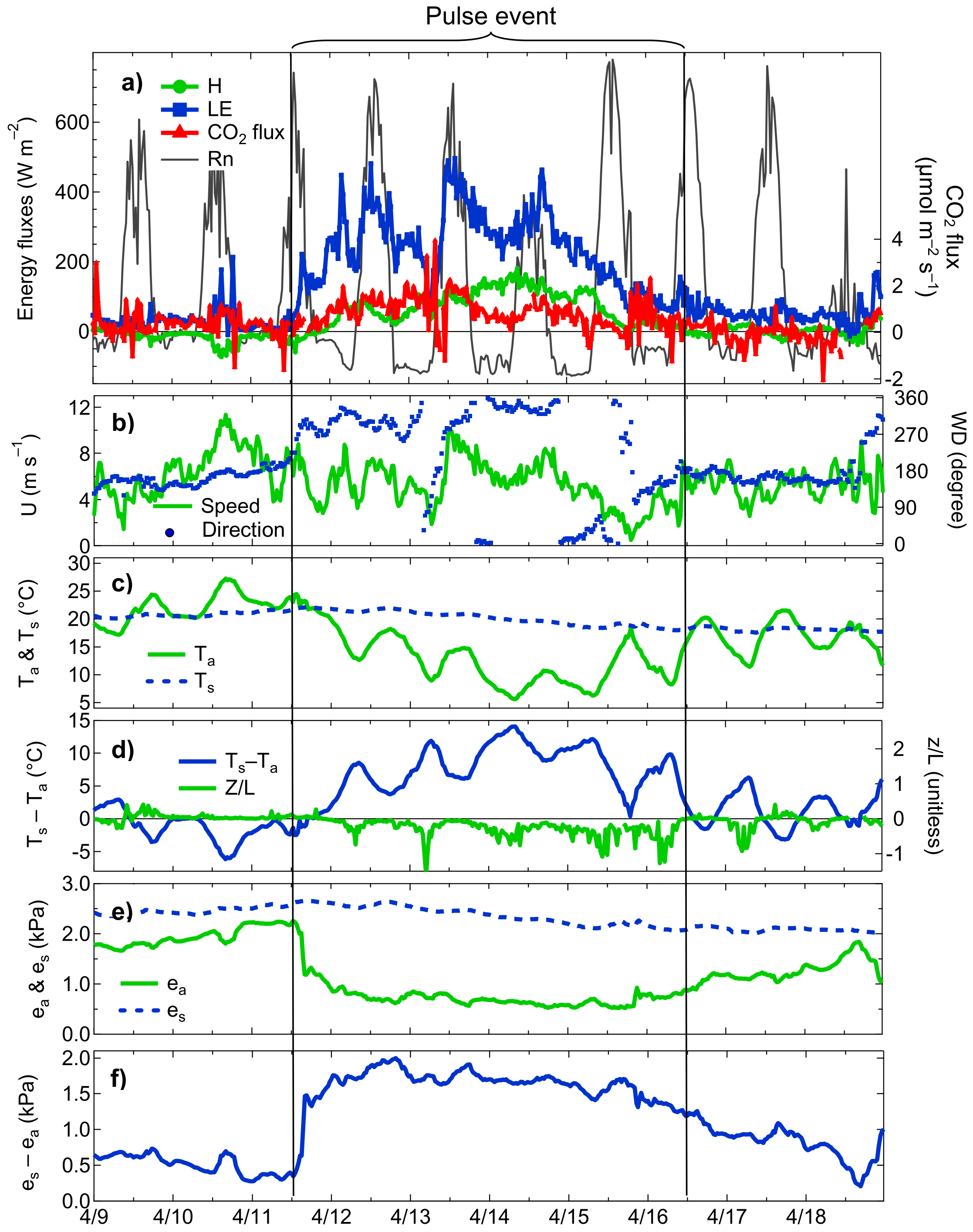

Figure 3. Changes in the surface energy budget components and meteorological variables after a cold front passage. The flux pulse started at approximately 12:00 LT on 11 April 2008 and ended on 16 April 2008. (a) *H*: sensible heat flux (W m^{-2}); LE: latent heat flux (W m^{-2}); Rn: net radiation (W m^{-2}); and CO_2 flux (μmol m^{-2} s^{-1}). (b) *U*: wind speeds (m s^{-1}); WD: wind direction in degree. (c), T_a: air temperature (°C); T_s: water surface temperature (°C). (d) T_s—T_a (°C); $\zeta = z/L$: atmospheric stability parameter with *z* being the distance above the water surface and *L* being the Obukhov length; (e) e_a: vapor pressure (kPa) in the over-water atmosphere; e_s: saturation vapor pressure in the water-air interface (kPa). (f) e_s—e_a (kPa).

and vapor pressure from 2.2 to 0.6 kPa. Cold, dry air masses passing over the warm water surface enhanced temperature and humidity differences between the underlying water surface and the overlying atmosphere (i.e., an increase in T_s—T_a and e_s—e_a), thereby enhancing convective mixing as reflected by the unstable stratification, and the windy conditions increased mechanical mixing, as compared with the pre- and post-pulse conditions. As a consequence, pulses in H, LE, and CO_2 fluxes were produced. The mean fluxes during the pulse period were approximately −10, 6, and 5 times the pre- and post- pulse averaged fluxes, respectively for H, LE, and CO_2 fluxes.

Driven by higher wind speeds and thus greater atmospheric mechanical turbulence, the friction velocity (u_*) during the pulse period was approximately

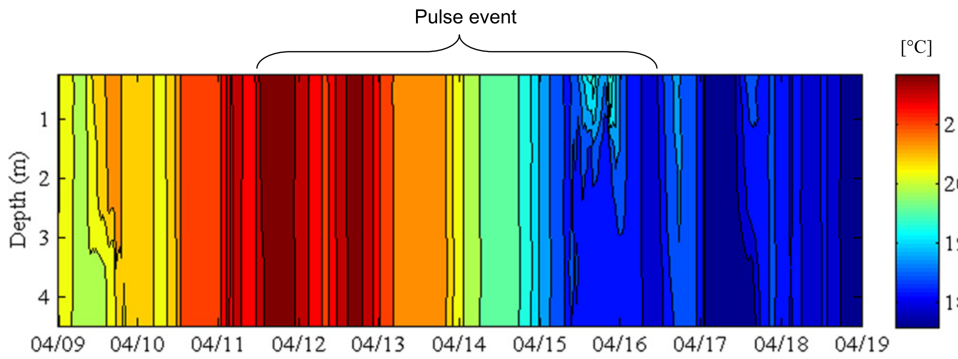

Figure 4. Changes in the water thermal structure during the same period in figure 3. The flux pulse started at approximately 12:00 LT on 11 April 2008 and ended on 16 April 2008.

Table 1. Contributions of pulse events to CO_2 fluxes and meteorological variables in 2008.

	Days	CO_2 flux μmol m^{-2} s^{-1}	U m s^{-1}	T_a °C	T_s °C	e_a kPa	e_s kPa	T_s—T_a °C	e_s—e_a kPa
All[a]	365	0.31	3.83	17.9	20.3	1.55	2.60	2.4	1.05
NPs	307	0.26	3.58	19.1	20.9	1.66	2.69	1.7	1.02
Ps	58	0.47	5.14	11.3	17.1	0.94	2.11	5.8	1.17
%	N/A	16.1	7.5%	−6.7%	−2.9%	−7.1%	−3.5%	28.0%	2.9%

[a] NPs: non-pulse; Ps: pulse; U: wind speeds (m s^{-1}); T_a: air temperature (°C); T_s: water surface temperature (°C); e_a: vapor pressure in the over-water atmosphere (kPa); e_s: saturation vapor pressure in the water-air interface (kPa); %: percentage of the pulse contribution to CO_2 fluxes (μmol^{-1} m^{-2} s^{-1}) and other meteorological variables.

48% greater than during non-pulse periods, so it combined with cooling to lead to an efficient mixing in the water column. As the water column was well mixed to the depth of the sensors during the pulse event shown here, the Wedderburn number could not be calculated. During pulse events in the more stratified period, the upwelling, internal wave induced mixing, and mixing by convection likely co-occurred as in figure 4. Under these circumstances, CO_2-rich near bottom waters were likely to be brought up to the water surface during the pulse period, leading to substantially larger CO_2 effluxes, as compared with non-pulse periods.

A total of 38 flux pulses were identified for 2008, covering 58 days throughout the year (16% of the year) (table 1). A total of 36 pulses were also identified for 2009, covering 57 days (Zhang and Liu 2013). On average, pulses covered approximately 22% of the days in the cool season from October to March and 9% of the days in the warm season from April to September (Zhang and Liu 2013). There were 2–4 pulses per month in the cool season and each pulse persisted 2–5 days; whereas there were 1–2 pulses per month in the warm season and each pulse persisted 2–3 days. Measured annual CO_2 efflux of 0.31 μmol m^{-2} s^{-1} (i.e., 431 g CO_2 m^{-2} yr^{-1}) would have been reduced to 0.26 μmol m^{-2} s^{-1} (i.e., 362 g CO_2 m^{-2} yr^{-1}) if CO_2 flux pulses were excluded. The flux pulses, which occurred during windy and stormy days, increased annual CO_2 effluxes by 16% in this study. CO_2 effluxes estimated by indirect methods are based on aquatic pCO_2 measurements. Any missing field sampling during these inclement weather conditions inherently exclude direct impacts of pulse events on CO_2 effluxes. As a consequence, the conventional indirect methods would likely underestimate CO_2 emission rates if sampling is inadequate during stormy days and thus pulse events and the enhanced CO_2 effluxes are under-sampled (table 1).

3.3. Implications of greater nighttime effluxes and flux pulses to carbon emissions

Short-term eddy covariance measurements also reported greater CO_2 effluxes at night than during daytime over Toolik Lake (68°37.91′N, 149°36.32′W) in Alaska, USA, Soppensee Lake (47°05.46′N, 8°05.00′E) in Switzerland for several days (Eugster *et al* 2003), and in the equatorial Pacific (3°S, 125°W) for 15 days (McGillis *et al* 2004). Methane fluxes are also observed to be greater at night than during the day over an Amazon floodplain (Crill *et al* 1988) and over a Swedish lake (60°09′N, 17°20′) for 16 days (Podgrajsek *et al* 2014). This suggests that the greater carbon effluxes from water surfaces at night than during the day may be widespread. Year-round eddy covariance studies of lake-atmosphere interactions have increased over the past years (Vesala *et al* 2006, Blanken *et al* 2011, Huotari *et al* 2011, Nordbo *et al* 2011, Bouin *et al* 2012, Liu *et al* 2012, Zhang and Liu 2013). Also, diel cycles of stratification and mixing are well established for lakes at many latitudes (Melack and Kilham 1974, Imberger 1985, Xenoupolis and Schindler 2001, MacIntyre *et al* 2002, 2009a, Pernica *et al* 2014). These similarities indicate that the physical processes that moderate all lakes are similar with some variability likely in forcing terms as a function of latitude. Thus, the framework proposed here to evaluate periods with intensified gas fluxes applies to other inland water bodies.

If the enhanced nocturnal and pulse induced fluxes reported here are representative of those over lakes and reservoirs, our results imply that CO_2 emission rates from lakes and reservoirs obtained by indirect measurements are substantially underestimated. For our case, estimated fluxes would be approximately 42% too low. Our 42% estimate is conservative because the indirect methods consistently obtain overall lower CO_2 fluxes than the eddy covariance approach even during the daytime (Huotari *et al* 2011, Heiskanen *et al* 2014). Further, this reservoir is managed for reducing algal abundance by, e.g., water cleaning practices and enacting regulations. Many lakes without such management as well as more eutrophic water bodies, in general, would have higher levels of phytoplankton, higher photosynthesis during the daytime in the near surface, and higher respiration lower in the water column much of the time, leading to larger diel variations in pCO_2. Thus, the contrast in CO_2 efflux between day and night is likely to be even larger for these unmanaged systems.

H and *LE* flux pulses have been reported from other inland waters with different water surface areas and in different latitudes, including Great Slave Lake (Blanken *et al* 2000), a reservoir in southeast Queensland, Australia (McGloin *et al* 2014), a tropical reservoir (Curtarelli *et al* 2013), a medium-sized Mediterranean lagoon (Bouin *et al* 2012), a large southern lake in China (Deng *et al* 2013), Lake Ngoring over Tibetan Plateau (Li *et al* 2015), and an ocean gulf in China (Ma *et al* 2012), suggesting that the phenomenon is widespread. The CO_2 flux pulses were also observed in a small lake in Finland, though the reasons for these pulses were not analyzed (Huotari *et al* 2011). It is likely that flux pulse events are associated with a generic response of water bodies to persistent extratropical cyclone activities. One projection is that extratropical cyclone activity will be intensified under future climate change (Lambert and Fyfe 2006, Ulbrich *et al* 2009), consequently leading to increased CO_2 flux pulses from lakes and reservoirs. Accordingly, insufficient pCO_2 sampling of surface waters during pulse periods will bias CO_2 emissions low when fluxes are computed based on the indirect methods.

The global terrestrial land surface is an important carbon sink (Battin *et al* 2009, Ballantyne *et al* 2012). A significant part of this organic carbon initially sequestered as CO_2 by terrestrial ecosystems is laterally transported to inland waters (Battin *et al* 2009, Regnier *et al* 2013). A large fraction (approximately 30%) of the terrestrially sequestered carbon entering inland waters is emitted as CO_2 back to the atmosphere (Kling *et al* 1991, Cole *et al* 2007, Battin *et al* 2009, Raymond *et al* 2013). Thus, emissions from lakes and other inland waters can represent a missing component of the terrestrial sink (Cole *et al* 2013). Measurements reported here suggest that terrestrially derived CO_2 that outgases to the atmosphere through lakes and reservoirs may be greater than previously estimated due to the unaccounted for greater nighttime emissions and inadequate sampling of flux pulses during synoptic weather events. Therefore the terrestrial carbon sink, which is likely attributed to rising atmospheric CO_2 and nitrogen deposition, may have been substantially overestimated.

4. Conclusions

If sampled only during fair weather daytime conditions, our measurements indicate that CO_2 effluxes from Ross Barnett reservoir would be underestimated by about 42%. Consequently, these results suggest that published estimates of CO_2 emission rates from inland waters, using indirect methods are biased low due to insufficient sampling during night and during storm events. The findings here provide a blue-print on how to construct a conditional sampling framework that reduces potential biases when upscaling local inland water fluxes to regional budgets for CO_2 and CH_4.

Acknowledgments

HL and QZ acknowledge support by National Science Foundation AGS under grant 1112938. GK acknowledges support from the National Science Foundation (NSF-EAR-1344703) and the US Department of Energy through the Office of Biological and Environmental ResearchTerrestrial Carbon Processes program (DE-SC0006967 and DE-SC0011461). SM acknowledges NSF DEB 0919603. We thank Dan Gaillet, Billy Lester, Jason Temple, and staff in Pearl River Valley Water Supply District in Ridgeland, Mississippi, as well as Yu Zhang, Haimei Jiang, Li Sheng, Rongping Li, Yu Wang, and Guo Zhang who contributed to field work.

We thank Zhongming Gao for his help in preparing this manuscript. We also thank the anonymous reviewers and one ERL board member for their constructive comments that greatly improved this manuscript.

References

Åberg J, Jansson M and Jonsson A 2010 Importance of water temperature and thermal stratification dynamics for temporal variation of surface water CO_2 in a boreal lake *J. Geophys. Res.* **115** G02024

Ballantyne A P, Alden C B, Miller J B, Tans P P and White J W C 2012 Increase in observed net carbon dioxide uptake by land and oceans during the past 50 years *Nature* **488** 70–2

Bastviken D, Tranvik L J, Downing J A, Crill P M and Enrich-Prast A 2011 Freshwater methane emissions offset the continental carbon sink *Science* **331** 50

Battin T J *et al* 2009 The boundless carbon cycle *Nat. Geosci.* **2** 598–600
Blanken P D *et al* 2000 Eddy covariance measurements of evaporation from Great Slave Lake, Northwest Territories, Canada *Water Resour. Res.* **36** 1069–77
Blanken P D, Spence C, Hedstrom N and Lenters J D 2011 Evaporation from lake superior: 1. Physical controls and processes *J. Great Lakes Res.* **37** 707–16
Bouin M-N, Caniaux G, Traullé O, Legain D and Le Moigne P 2012 Long-term heat exchanges over a Mediterranean lagoon *J. Geophys. Res.* **117** D23104
Cole J J *et al* 2007 Plumbing the global carbon cycle: integrating inland waters into the terrestrial carbon budget *Ecosystems* **10** 171–84
Cole J J, Bade D L, Bastviken D, Pace M L and Van de Bogert M 2010 Multiple approaches to estimating air-water gas exchange in small lakes *Limnol. Oceanogr. Methods* **8** 285–93
Cole J J, Caraco N F, Kling G W and Kratz T K 1994 Carbon dioxide supersaturation in the surface waters of lakes *Science* **265** 1568–70
Cole J J, Kinne O, Reynolds C S and Seaman M N 2013 *Freshwater Ecosystems and the Carbon Cycle* (International Ecology Institute) 146
Crill P *et al* 1988 Trophospheric methane from an Amazon floodplain lake *J. Geophys. Res.* **93** 1564–70
Curtarelli M P, Alcântara E H, Rennó C D and Stech J L 2013 Modeling the effects of cold front passages on the heat fluxes and thermal structure of a tropical hydroelectric reservoir *Hydrol. Earth Syst. Sci. Discuss* **10** 8467
Deng B *et al* 2013 Evaluation of the CLM4 lake model at a large and shallow freshwater lake *J Hydrometeor.* **14** 636–49
Eugster W *et al* 2003 CO_2 exchange between air and water in an Arctic Alaskan and midlatitude Swiss lake: importance of convective mixing *J. Geophys. Res.* **108** 4362
Heiskanen J J, Mammarella I, Haapanala S, Pumpanen J, Vesala T, MacIntyre S and Ojala A 2014 Effects of cooling and internal wave motions on gas transfer coefficients in a boreal lake *Tellus* B **66** 22827
Huotari J *et al* 2011 Long-term direct CO_2 flux measurements over a boreal lake: five years of eddy covariance data *Geophys. Res. Lett.* **38** L18401
Imberger J 1985 The diurnal mixed layer *Limnol. Oceanogr.* **30** 737–70
Imberger J and Patterson J C 1990 Physical limnology *Adv. Appl. Mech.* **27** 303–475
Jeffery C, Woolf D, Robinson I and Donlon C 2007 One-dimensional modelling of convective CO_2 exchange in the tropical Atlantic *Ocean Modell.* **19** 161–82
Jonsson A, Åberg J, Lindroth A and Jansson M 2008 Gas transfer rate and CO_2 flux between an unproductive lake and the atmosphere in northern Sweden *J. Geophys. Res.* **113** G04006
Kling G W, Kipphut G W and Miller M C 1991 Arctic lakes and streams as gas conduits to the atmosphere: implications for tundra carbon budgets *Science* **251** 298–301
Lambert S J and Fyfe J C 2006 Changes in winter cyclone frequencies and strengths simulated in enhanced greenhouse warming experiments: results from the models participating in the IPCC diagnostic exercise *Clim. Dyn.* **26** 713–28
Li Z, Lyu S, Ao Y, Wen L, Zhao L and Wang S 2015 Long-term energy flux and radiation balance observations over Lake Ngoring, Tibetan Plateau *Atmos. Res.* **155** 13–25
Liu H *et al* 2009 Eddy covariance measurements of surface energy budget and evaporation in a cool season over southern open water in Mississippi *J. Geophys. Res.* **114** D04110
Liu H *et al* 2011 Variability in cold front activities modulating cool-season evaporation from a southern inland water in the USA *Environ. Res. Lett.* **6** 024022
Liu H, Zhang Q and Dowler G 2012 Environmental controls on the surface energy budget over a large southern inland water in the United States: an analysis of one-year eddy covariance flux data *J. Hydrometeor.* **13** 1893–910
Ma Y, Huang F, Huang J and Wang H 2012 Observational study on heat flux in the coastal zone of Pearl River mouth in spring 2006 *J. Tropical Oceanogr.* **31** 49–57
MacIntyre S *et al* 2009a Climate-related variations in mixing dynamics in an Alaskan arctic lake *Limnol. Oceanogr.* **54** 2401
MacIntyre S, Clark J F, Jellison R J and Fram J P 2009b Turbulent mixing induced by non-linear internal waves in Mono Lake, CA *Limnol. Oceanogr.* **54** 2255–72
MacIntyre S *et al* 2010 Buoyancy flux, turbulence, and the gas transfer coefficient in a stratified lake *Geophys. Res. Lett.* **37** L24604
MacIntyre S, Romero J R and Kling G W 2002 Spatial-temporal variability in surface layer deepening and lateral advection in an embayment of Lake Victoria, East Africa *Limnol. Oceanogr.* **47** 656–71
McGillis W R *et al* 2004 Air-sea CO_2 exchange in the equatorial Pacific *J. Geophys. Res.* **109** C08S02
McGloin R, McGowan H and McJannet D 2014 Effects of diurnal, intra-seasonal and seasonal climate variability on the energy balance of a small subtropical reservoir *Int. J. Climatol.* **35** 2308–25
Melack J M and Kilham P 1974 Photosynthetic rates of phytoplankton in East African alkaline, saline lakes *Limnol. Oceanogr.* **19** 743–55
Nordbo A *et al* 2011 Long-term energy flux measurements and energy balance over a small boreal lake using eddy covariance technique *J. Geophys. Res.* **116** D02119
Pernica P, Wells M G and MacIntyre S 2014 Persistent weak thermal stratification inhibits mixing in the epilimnion of north-temperate Lake Opeongo, Canada *Aquatic Sci.* **76** 187–201
Podgrajsek E, Sahlée E and Rutgersson A 2014 Diurnal cycle of lake methane flux *J. Geophys. Res. Biogeosci.* **119** 236–48
Raymond P A *et al* 2013 Global carbon dioxide emissions from inland waters *Nature* **503** 355–9
Regnier P *et al* 2013 Anthropogenic perturbation of the carbon fluxes from land to ocean *Nat. Geosci.* **6** 597–607
Rutgersson A and Smedman A 2010 Enhanced air-sea CO_2 transfer due to water-side convection *J. Marine Sys.* **80** 125–34
Rutgersson A, Smedman A and Sahlée E 2011 Oceanic convective mixing and the impact on air-sea gas transfer velocity *Geophys. Res. Lett.* **38** L02602
Sobek S, Tranvik L J and Cole J J 2005 Temperature independence of carbon dioxide supersaturation in global lakes *Global Biogeochem. Cycles* **19** GB2003
Sobolev D, Moore K and Morris A L 2009 Nutrients and light limitation of phytoplankton biomass in a turbid southeastern reservoir: implications for water quality *Southeastern Naturalist* **8** 255–66
Tranvik L J *et al* 2009 Lakes and reservoirs as regulators of carbon cycling and climate *Limnol. Oceanogr.* **54** 2298–314
Ulbrich U, Leckebusch G C and Pinto J G 2009 Extra-tropical cyclones in the present and future climate: a review *Theore. Appl. Climat.* **96** 117–31
Vesala T *et al* 2006 Eddy covariance measurements of carbon exchange and latent and sensible heat fluxes over a boreal lake for a full open-water period *J. Geophys. Res.* **111** D11101
Wersal R M, Madsen J D and Tagert M L 2006 Aquatic plant survey of Ross Barnett Reservoir for 2005 *Tech. Rep.* Mississippi State University, Mississippi
Xenopoulos M A and Schindler D W 2001 The environmental control of near-surface thermoclines in boreal lakes *Ecosys.* **4** 699–707
Zappa C J, Asher W E, Jessup A T, Klinke J and Long S R 2004 Microbreaking and the enhancement of air-water transfer velocity *J. Geophys. Res.* **109** C08S16
Zhang Q and Liu H 2013 Interannual variability in the surface energy budget and evaporation over a large southern inland water in the United States *J. Geophys. Res.* **118** 4290–302
Zhang Q and Liu H 2014 Seasonal changes in physical processes controlling evaporation over inland water *J. Geophys. Res.* **119** 9779–92